

Article

Study of Al–SiO₂ Aesthetic Composite Coating on Orthodontic Metal Archwire

Haopeng Wu ¹, Jie Yang ¹, Yuwen Yan ¹, Bowen Zheng ¹, Ahmed Lotf Algahefi ¹, Song Ma ² and Yi Liu ^{1,*} 

¹ Liaoning Provincial Key Laboratory of Oral Diseases, School and Hospital of Stomatology, China Medical University, Shenyang 110002, China; 2020121585@cmu.edu.cn (H.W.); 2021121763@cmu.edu.cn (J.Y.); ywyan@cmu.edu.cn (Y.Y.); bwzheng@cmu.edu.cn (B.Z.); 2019231002@cmu.edu.cn (A.L.A.)

² Shenyang National Laboratory for Materials Science, Institute of Metal Research, Chinese Academy of Sciences, Shenyang 110016, China; songma@imr.ac.cn

* Correspondence: liuyi@cmu.edu.cn; Tel.: +86-24-3197-3999

Abstract: Nickel–titanium orthodontic wires (NTWs) play an essential role in orthodontic treatment. However, their corrosion and aesthetic properties limit their applications. To improve the aesthetic effects of nickel–titanium orthodontic archwires, we prepared aluminium–silicon dioxide (Al–SiO₂) as a biocompatible layer coated onto the NTWs. The Al–SiO₂ coating was first fabricated using physical vapor deposition magnetron sputtering, and its physicochemical and biocompatibility properties were investigated. Al–SiO₂ layers were well coated on the NTWs. The corrosion currents in the nickel–titanium (NiTi) control, Al–SiO₂-coated NiTi experimental, stainless steel (SS) control and Al–SiO₂-coated SS experimental groups were 23.72 $\mu\text{A cm}^{-2}$, 1.21 $\mu\text{A cm}^{-2}$, 0.22 $\mu\text{A cm}^{-2}$ and 0.06 $\mu\text{A cm}^{-2}$, respectively. Al–SiO₂-coated NTWs with reduced corrosion current density indicated that the preparation of Al–SiO₂ coating on the surface of NiTi and SS could reduce the tendency of electrochemical corrosion. The friction coefficients of orthodontic wires in the NiTi control, NiTi experimental, SS control, and SS experimental groups were 0.68, 0.46, 0.58 and 0.45, respectively. A low friction coefficient was observed in the Al–SiO₂-coated NTWs, and the reduced friction coefficient improved the efficiency of orthodontics. Furthermore, the excellent biocompatibility of the NTWs and SS coated with Al–SiO₂ indicates that Al–SiO₂ as a novel aesthetic layer could improve the physicochemical properties of NTW and SS without causing cytotoxicity, which has considerable potential for modification of NTW and SS surfaces.

Keywords: aluminum–silicon dioxide; surface modification; corrosion; archwire; aesthetic



Citation: Wu, H.; Yang, J.; Yan, Y.; Zheng, B.; Algahefi, A.L.; Ma, S.; Liu, Y. Study of Al–SiO₂ Aesthetic Composite Coating on Orthodontic Metal Archwire. *Coatings* **2022**, *12*, 746. <https://doi.org/10.3390/coatings12060746>

Academic Editor: Ludmila B. Boinovich

Received: 26 April 2022

Accepted: 26 May 2022

Published: 29 May 2022

Publisher's Note: MDPI stays neutral with regard to jurisdictional claims in published maps and institutional affiliations.



Copyright: © 2022 by the authors. Licensee MDPI, Basel, Switzerland. This article is an open access article distributed under the terms and conditions of the Creative Commons Attribution (CC BY) license (<https://creativecommons.org/licenses/by/4.0/>).

1. Introduction

Brackets and archwires are two major parts of fixed appliances. In detail, brackets can align teeth under continuous forces exerted by the archwires. Although several aesthetic appliances have been utilized in orthodontic treatment, stainless steel (SS) brackets and nickel-titanium wires (NTWs) are still the most commonly used in clinical treatment [1].

Metal materials are vulnerable to corrosion when exposed to air or water [2], let alone the oral cavity, which is an extremely complex environment and easily affected by saliva, bacterial flora, food, temperature fluctuations and mechanical forces. Corrosion can increase the surface roughness of the metal surface, resulting in increased friction forces between the archwire and the bracket and subsequently hindering teeth movement. Additionally, the increased friction can accelerate the corrosion process under continuously increasing stress [3,4].

There are many kinds of commercially available aesthetic coatings. For example, rhodium coating, epoxy coating, polytetrafluoride coating, platinum and silver coating, and polymer coating [5–8] have inherent limitations and are therefore not widely used in clinical practice. Alsanea et al. [5] investigated the color stability of rhodium, epoxy resin, and

polytetrafluoroethylene nickel titanium aesthetic coatings. They found that the archwires of polytetrafluoron coating, epoxy resin coating and rhodium aesthetic coating all changed after being immersed in a dyeing solution for 4 weeks, among which the polytetrafluoron coating changed most markedly. Pezzato et al. [9] evaluated the tribocorrosion behavior of plasma electrolytic oxide-coated AZ91 samples. Magnesium alloys are characterized by low wear resistance and poor corrosion resistance. After plasma electrolytic oxidation, the tribocorrosion performance was markedly improved, indicating that the addition of the coating to the alloy surface can obviously improve the material properties. Rachele et al. [10] examined that wear and corrosion-caused metal ion release shortens the lifespan of a prosthesis. Cryogenic machining weakens the corrosion and fretting corrosion performance of the additive Ti6Al4V. Polyether ether ketone is a high-temperature thermoplastic polymer composed of aromatic main chain molecules connecting ketone and ether functional groups and has been used in the development of orthodontic archwire coating. Although it is cosmetically appealing, more studies are needed to determine its physical properties [6]. Researchers and clinicians have found that the current clinical aesthetic archwire coating is prone to damage under the masticatory force and oral salivary enzymes, along with color changes over time. Moreover, the archwire coating cracks and detaches during the force application, thus exposing the inner metal, increasing the surface roughness and further affecting the correction process [7,8]. Hence, development of archwires with stable coating properties and a certain level of corrosion or friction resistance is gaining interest in orthodontic treatment.

Aluminum (Al), the most abundant metal element on the planet, is widely used in biomedical materials. Silicon dioxide (SiO_2) is a common modification layer given its superior physicochemical stability and biocompatibility. Importantly, the oxide layer may obstruct ion movement and release, improving metal mechanical properties and stability [11].

Magnetron sputtering can produce a uniform, smooth coating on the substrate surface. SiO_2 is applied in many fields due to its rich properties, low cost, good chemical stability, and strong physical properties such as biocompatibility, high mechanical strength, wear resistance, corrosion resistance, hydrophobicity and high optical transparency [12–14]. The oxide layer can inhibit the outward movement of ions, thus becoming a barrier to ion release and playing a protective role against material decomposition [15–17]. SiO_2 is widely used in metal protective coatings on metals and in biomedical and biotechnological applications while showing great potential in enzymes and metal catalysis, drugs, genes, protein transport, biological imaging, pollution repair, chromatography, and vector or carrier platforms for sensors and structural templates [14,18]. There are various methods for film preparation, such as micro-arc oxidation, physical vapor deposition magnetron sputtering (PVDMS), plasma spray, chemical vapor deposition, solvent-gel coating, ion beam-assisted deposition, and pulsed laser deposition [15,19–25]. Among them, magnetron sputtering is widely used to prepare SiO_2 thin films, and the silica thin films produced through this process are transparent. Magnetron sputtering has many advantages: (i) strong binding force of coating and substrate; (ii) good metal surface uniformity; (iii) high deposition rate; (iv) high purity film; (v) easy to automate and high reproducibility; (vi) easy to sputter many metals and alloys; (vii) controllable film thickness; and (viii) low cost [5,17,26].

Considering the advantages of Al and SiO_2 , we prepared a novel modified layer based on the Al- SiO_2 composite and explored its potential application in fixed appliances. In detail, the Al- SiO_2 coating layer was first fabricated by PVDMS. Its physicochemical properties were evaluated utilizing scanning electron microscopy (SEM), energy dispersive spectroscopy (EDS), electrochemical corrosion and friction analysis [15,16,27,28]. Mouse fibroblasts were used to investigate the biocompatibility of Al- SiO_2 -coated samples.

Herein, we demonstrated the newly developed Al- SiO_2 coated NiTi and SS archwires using PVDMS. The morphology of the Al- SiO_2 coating was systematically characterized and its corrosion resistance was electrochemically assessed. Meanwhile, the wear and scratch tests were performed to confirm the friction coefficient and bonding strength. The

biocompatibility properties were also investigated. This work aimed to confirm that the Al-SiO₂ aesthetic composite coating was prepared based on the aesthetic appearance of Al coating and the corrosion resistance, low friction and wear resistance of silica to realize the combination of aesthetics with function.

2. Materials and Methods

2.1. Preparation and Characterization of Al-SiO₂-Coated Samples

Commercial orthodontic SS archwires and NiTi archwires (NTA) were selected as substrates (Shanghai Emundi, 0.016 × 0.022 inch, Shanghai, China). Nearly equiatomic NTA consists of Ni (55 wt.%) and Ti. It is a special shape memory alloy that can automatically restore its own plastic deformation to its original shape at a specific temperature [29]. Moreover, 2 × 2 × 0.2 cm³ SS archwire and NTA samples were prepared for further research. Before delivery, the cross-sections were ground using 600-, 1000-, 1500- and 2000-grit silicon carbide (SiC) paper to remove the oxide layer. As it was mechanically polished, only 2.5 μm diamond grinding paste is used for further polishing. They were ultrasonically cleaned with acetone and alcohol for 15–20 min and blow-dried with argon.

An unbalanced magnetron sputtering coating system was employed. Figure 1 presents the schematic diagram of PVDMS process. The distance between the target materials and the specimen was 7 cm. Argon gas could be passed into the vacuum chamber when the pressure value in the vacuum was lower than 3×10^{-3} Pa. This sequentially initiated the process of pre-sputtering of the target with the following parameters: pressure, 0.5 Pa; pre-sputtering time, 15 min; time required for Al deposition, 10 min; SiO₂ deposition time, 150 min; pulse voltage, 350 V; duty cycle, 15%; substrate voltage, 340 V; and deposition temperature, 250 °C.

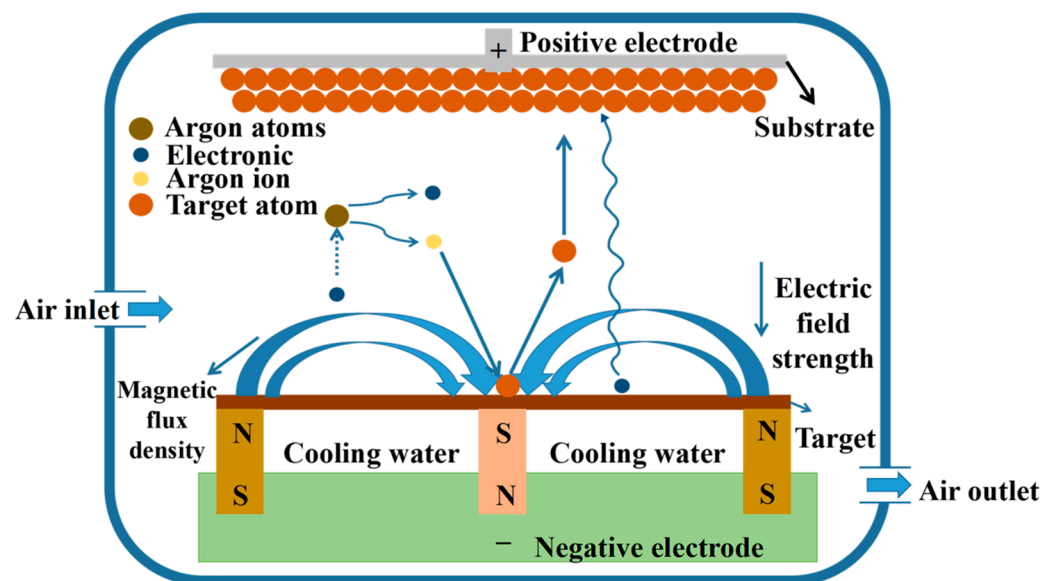


Figure 1. The schematic diagram of the physical vapor deposition magnetron sputtering process.

SEM characterized specimens' microstructure and surface morphology after gold spraying under vacuum pressure for 90 s. Additionally, the elemental composition of the coated layer was analyzed using EDS.

2.2. Cytotoxicity Tests

The cells used in this study were mouse fibroblasts NIH3T3. The experiment was divided into two groups: In the blank control group, uncoated SS archwires and Al-SiO₂ aesthetic SS archwires were used; in the blank control group, uncoated NiTi archwires and Al-SiO₂ aesthetic NiTi archwires were used. Mouse fibroblasts NIH3T3 were cultured at a density of 2×10^4 per sample for 1, 3, 5, and 7 days. Cell viability was evaluated using the

Cell Counting Kit-8 (CCK-8, Beyotime, Shanghai, China). The samples were washed twice with phosphate-buffered saline at each time point. Fresh culture medium (200 μL) was mixed with 20 μL of CCK-8 reagent and the mixture was added to each sample. Then, the culture was incubated at 37 $^{\circ}\text{C}$ for 2 h. Subsequently, 100 μL of the medium was transferred to a 96-well plate and absorbance was measured at 450 nm.

2.3. Electrochemical Corrosion Experiments

The electrochemical work station CHI760D (Reference 600, Gamry company, Warminster, PA, USA) was used to investigate the electrochemical performance of the coated layer. A conventional three-electrode setup was used for electrochemical measurement, with Pt as a counter electrode, standard Ag/AgCl as the control, and the anodized specimen as the working electrode. To simulate the human oral environment, artificial saliva was prepared and included the following components: 0.4 g/L NaCl, 0.4 g/L KCl, 0.906 g/L $\text{CaCl}_2 \cdot \text{H}_2\text{O}$, 0.69 g/L $\text{NaH}_2\text{PO}_4 \cdot 2\text{H}_2\text{O}$, 0.005 g/L $\text{Na}_2\text{S} \cdot 9\text{H}_2\text{O}$, and 1 g/L urea. Electrochemical tests were performed on the specimens in artificial saliva [30]. NiTi control, Al-SiO₂-coated NiTi experimental, SS control and Al-SiO₂-coated SS experimental groups were used. Uncoated surface was sealed with nail polish at room temperature. Dynamic polarization curves were recorded when open circuit potential was stable. Scanning speed was 0.33 $\text{mV} \cdot \text{s}^{-1}$, and scanning range was from -0.1 V to 1.5 V. E_{CORR} and its current density, i_{CORR} were defined from collected Tafel quantitative data.

2.4. Wear Test

A rotary friction and wear machine (Lanzhou Institute of Chemical Physics, Chinese Academy of Sciences) was used to investigate the friction and wear performance of the coated layers. The test conditions are presented in Table 1. The counterpart for the friction test was an Al₂O₃ ball with a diameter of 4 mm. The test was performed at room temperature in the NiTi control, Al-SiO₂-coated NiTi experimental, SS control and Al-SiO₂-coated SS experimental groups. The friction and wear of the coating were generally divided into three phases, namely the running-in phase, stable phase, and failure phase. Then, the average value of the friction coefficient in the stable phase was recorded as the friction coefficient of the coating.

Table 1. Process parameters for the wear test.

Friction Pairs	Load (N)	Turning Radius (mm)	Speed (r/min)	Test Time (min)
Alumina ball ($\varnothing = 4$ mm)	1	3	200	30

2.5. Scratch Test

The bonding strength of the coating layers was tested using an MFT-4000 scratch tester (Lanzhou Institute of Chemical Physics, Chinese Academy of Sciences, China). Test parameters were depicted as follows: radius, 0.2 ± 0.01 mm; scratch length, 5 mm; loading speed, 30 $\text{N} \cdot \text{min}^{-1}$; end load: 70 N. Scratch test was performed in the NiTi control, Al-SiO₂-coated NiTi experimental, SS control and Al-SiO₂-coated SS experimental groups.

2.6. Statistical Analysis

Statistical analysis was performed using SPSS 21.0 software (IBM Corporation, Armonk, NY, USA). All data are represented as mean \pm standard deviation. One-way analysis of variance (ANOVA) was used to evaluate the statistical significance among the four groups. A paired t-test was used to evaluate the differences between the two groups. A p -value of <0.05 was considered statistically significant. All experiments were performed in triplicate to ensure reproducibility.

3. Results

3.1. Coating Morphology Analysis

The cross-section and surface morphologies of the coating layers are shown in Figure 2. As shown in Figure 2a, the thickness of the coated layers was 1.8 μm . SEM findings regarding surface morphologies of Al-SiO₂-coated SS and Al-SiO₂-coated NiTi are shown in Figure 2b,c. All samples displayed uniform and dense layers securely attached to the substrate without any interfacial defects. Figure 2d shows the Al-SiO₂ coating, and its surface revealed a clear, smooth spherical structure. Al-SiO₂ coated on the SS and NiTi archwires is shown in Figure 2e,f, respectively. The color of the prepared aesthetic archwire was similar to that of the teeth, and the aesthetic effect was achieved.

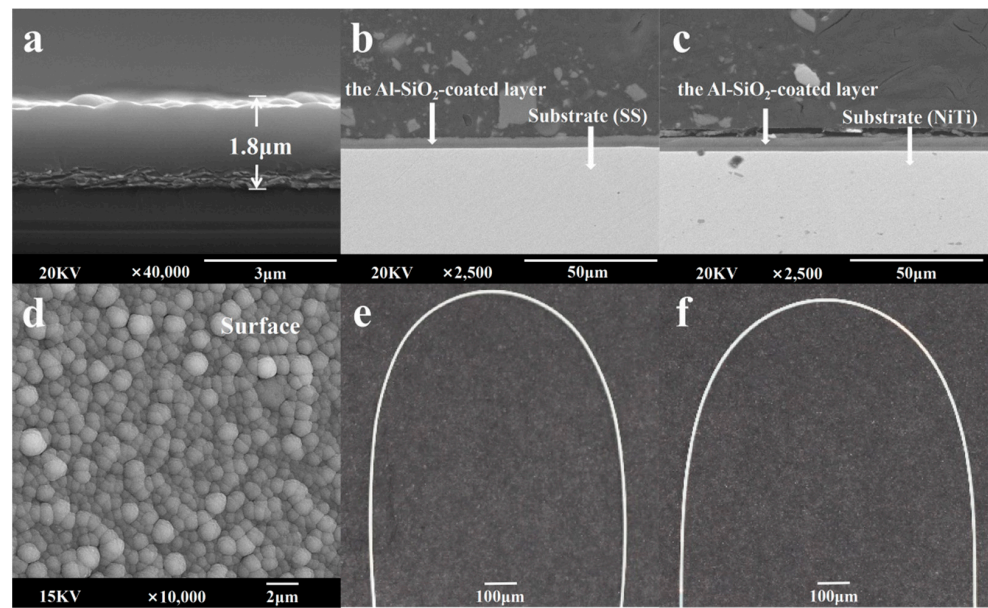


Figure 2. SEM observation of Al-SiO₂ coating and the macroscopic observation of archwire. Thickness of Al-SiO₂ coating layer (a); cross-section of the Al-SiO₂-coated SS (b); cross-section of the Al-SiO₂-coated NiTi (c); SEM findings regarding surface morphology of Al-SiO₂-coated layer (d); the macroscopic observation of NiTi archwire (e); the macroscopic observation of SS archwire (f).

3.2. EDS Analysis

Figure 3 shows the EDS findings of the particle distribution of the coatings. Uniform distribution of Al, O and Si elements was observed across the whole layer in the samples, which demonstrated that the Al-SiO₂ layers were well coated on the samples.

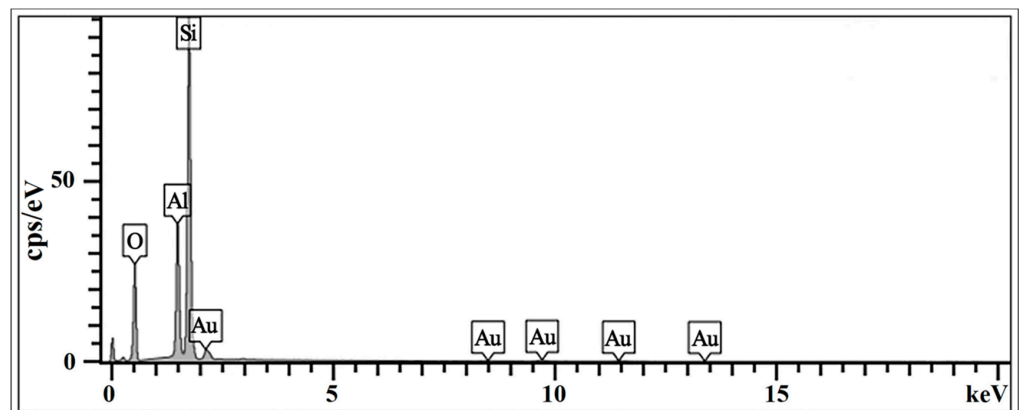


Figure 3. EDS mapping images of Al-SiO₂ coating.

3.3. Cytotoxicity

The cytotoxic level of the archwires was measured using a CCK-8 kit at 1, 3, 5, and 7 days (Figure 4). Statistical results showed that there was no significant difference in cytotoxic levels among the blank control, uncoated NiTi, and Al-SiO₂-coated NiTi groups. The three groups' optical density (OD) values increased with the increase in culture time, indicating that the cells grew well and preserved proliferation ability. Similarly, there was no significant difference in OD values among the other blank control, uncoated SS and Al-SiO₂-coated SS groups at 1, 3, 5, and 7 days and OD values in each of the three groups also increased with culture time. According to the cytotoxicity assessment, the OD values of the coated layer archwire in the experimental group were lower than those in the control group. The above results indicated no cytotoxicity of the coated archwire in the experimental group.

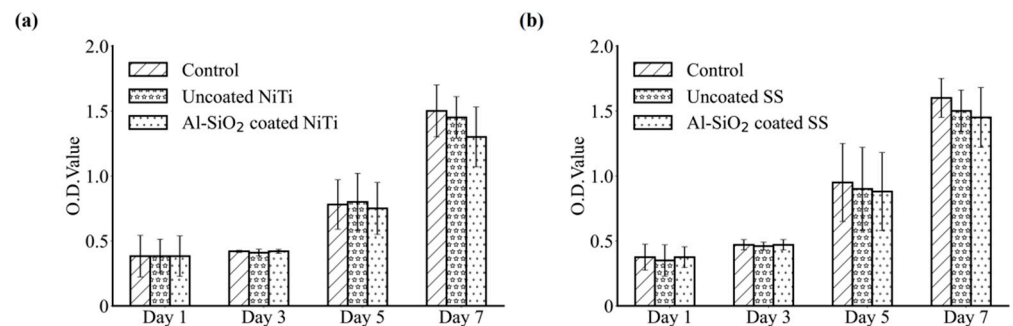


Figure 4. Cytotoxicity test for the coated archwires. Optical density values at different time points in the NiTi group (a). Optical density values of mouse fibroblasts at different time points in the SS group (b).

3.4. Electrochemical Corrosion Experiment

The results of the electrochemical experiments are shown in Figure 5. The corrosion currents in the NiTi control, NiTi experimental, SS control, and SS experimental groups were 23.72 $\mu\text{A cm}^{-2}$, 1.21 $\mu\text{A cm}^{-2}$, 0.22 $\mu\text{A cm}^{-2}$ and 0.06 $\mu\text{A cm}^{-2}$, respectively. The i_{corr} values decreased considerably from 23.72 $\mu\text{A cm}^{-2}$ to 1.21 $\mu\text{A cm}^{-2}$ while coating with Al-SiO₂ on the NiTi sample. Meanwhile, the i_{corr} value for Al-SiO₂ coated SS sample as 0.06 $\mu\text{A cm}^{-2}$ was lower than the SS sample of 0.22 $\mu\text{A cm}^{-2}$. The polarization current shows that the preparation of the Al-SiO₂ coating on the surface of NiTi and SS could reduce the tendency of electrochemical corrosion. Therefore, Tafel extrapolation results demonstrate that the Al-SiO₂ coating improved the corrosion resistance of the archwires. A summary of the electrochemical test quantitative data is shown in Table 2.

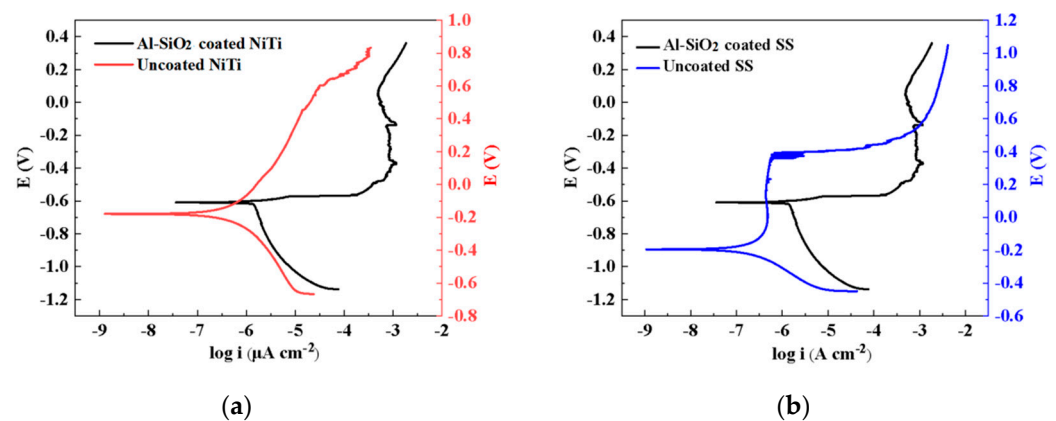


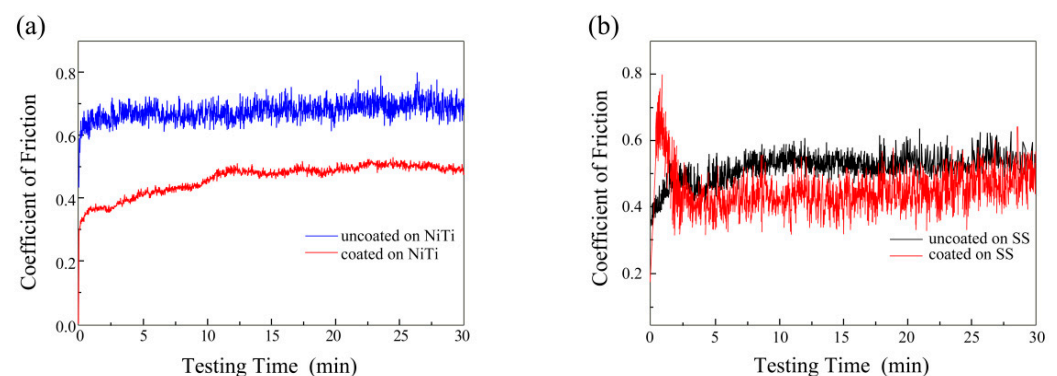
Figure 5. Electrochemical results for the coated archwires. Dynamic polarization curve of the NiTi group (a). Dynamic polarization curve of the SS group (b).

Table 2. Corrosion parameters from the polarization curves.

Sample	$E_{\text{corr}}/\text{V vs. SCE}$	$i_{\text{corr}}/\mu\text{A cm}^{-2}$
Uncoated NiTi	-0.18 ± 0.02	23.72 ± 4.99
Al-SiO ₂ -coated NiTi	-0.60 ± 0.08	1.21 ± 0.48
Uncoated SS	-0.20 ± 0.03	0.22 ± 0.09
Al-SiO ₂ -coated SS	-0.61 ± 0.10	0.06 ± 0.01

3.5. Friction and Wear Properties

The friction coefficient curve of the coated layers is shown in Figure 6. The recorded friction process was divided into two phases. In phase I, the friction coefficient changed over time, which was in the unstable running-in phase. In phase II, the friction coefficient tended to be stable. The mean value of the friction coefficient in the stable phase was recorded as the friction coefficient of the coating. NiTi control and experimental groups showed a steady-state friction coefficient after an initial 12 min of sliding, which indicated a transmission from phase I to phase II. The SS control and experimental groups showed a steady-state friction coefficient after an initial 9 min of sliding. The friction coefficients of the NiTi control and experimental groups, SS control and experimental groups were 0.68, 0.46, 0.58 and 0.45, respectively.

**Figure 6.** Friction coefficient curve of the coated layers. NiTi group (a); SS group (b).

3.6. Bonding Strength

The critical load (L_c) is at the peak of the curve, as shown in Figure 7. The position of the inflection point coincided with the location of the first acoustic signal, which corresponded to the L_c . The Al-SiO₂-coated NiTi archwire's and SS archwire's mean L_c values were 15.07 N and 8.3 N, respectively. High-vacuum plasma ion titanium sputtering was carried out on the NiTi archwires with a titanium disc (>99.9%) as the sputtering target material, according to the experiment by Anuradha et al. [31]. The coatings were found to be relatively stable in a linear scratch test when the L_c was >8 N. Therefore, 8 N was used as a control group to evaluate the binding force of the Al-SiO₂ coating. The Al-SiO₂ coatings were found to be relatively stable in the linear scratch test and could meet clinical requirements.

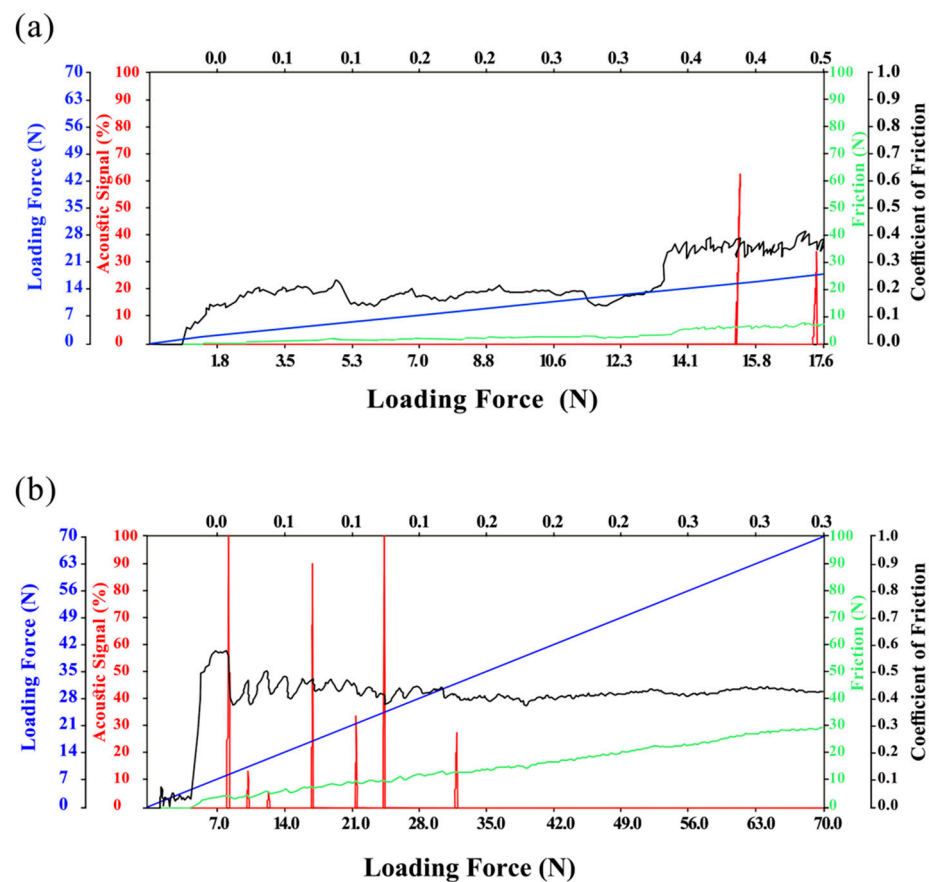


Figure 7. The scratch test of the coated archwires. The coating of NiTi specimen (a). The coating of SS specimen (b).

4. Discussion

For the development of esthetic dental appliances, orthodontic archwires must meet certain requirements before being used clinically; these include high strength, low friction, corrosion resistance, friction resistance, and biocompatibility [32]. Various coatings were developed to modify the surface of orthodontic archwires to improve their physicochemical and biological properties. In this study, Al-SiO₂-coated layers were used to create esthetic orthodontic archwires with good biocompatibility and physical properties.

The CCK-8 (cell counting kit-8) was tested at various time intervals (1, 3, 5, and 7 days) as shown in Figures 3 and 4. There was no significant difference in cytotoxicity between the Al-SiO₂ samples and the control group. Therefore, Al-SiO₂-coated layers could be considered safe and useful for clinical application.

Various substances in the mouth can cause electrochemical corrosion reactions on the surface of the archwires [33]. Since different metallic elements are present in the mouth, it may lead to electro-galvanic cell formation, which can contribute to corrosion. Microorganisms such as sulfate-reducing bacteria may also be present in the metabolic flora of the oral cavity, which can cause biological corrosion. Therefore, the presence of microorganisms can change the state of the biomaterial surface and accelerate the biological corrosion process [34]. The formation of biofilms leads to changes in oral cavity parameters including pH, electrolytic concentration and oxygen levels. Furthermore, there are three types of corrosive cells in the oral environment: cells with varying degrees of oxygenation, cells containing different concentrations of metal ions and active-passive cells [34–36]. Currently, the corrosion resistance of aesthetic archwires in clinical practice needs further improvement. The rhodium coating is aesthetically pleasing but has low corrosion resistance, which may be due to galvanic coupling between the noble coating and the base alloy [37]. Previous literature has investigated polymer coatings such as epoxy

resins, which reduce the corrosion resistance of archwires compared to uncoated NiTi and SS archwires [38]. Therefore, it is urgent to produce orthodontic archwires with a high level of corrosion resistance. The current findings demonstrated that Al-SiO₂ coatings could reduce the corrosion rates of NiTi and SS archwires in artificial saliva through polarization curves, which were achieved from corrosion tests. The microstructures and compositions of the Al-SiO₂ coatings with a smooth surface are uniform and could well protect the surface of the archwires.

To the best of our knowledge, the presence of friction may have affected the efficiency of tooth movement during fixed orthodontic treatment. Kusy et al. [39] demonstrated that friction could reduce 12%–60% of the orthodontic force during orthodontic treatment, influencing clinical treatment. Previous research has verified that certain aesthetic-coated archwires can increase the roughness [40]. Moreover, some studies have investigated the microscopic observations of uncoated archwires and rhodium-coated aesthetic archwires. The results show that rhodium archwires increase the roughness of NiTi archwires [31,40]. Another study found that the surface roughness of rhodium-coated archwires was similar to that of uncoated archwires [31]. However, compared to uncoated archwires, Teflon- and epoxy-coated archwires showed a significant difference in surface roughness. The surface roughness of the epoxy coating was reported to be higher than that of the Teflon coating [5]. The latter can meet aesthetic requirements; however, the coating's surface roughness is unacceptable. The friction coefficients of Al-SiO₂-coated SS and NiTi archwires were lower than those of uncoated groups, according to the wear test results in this study. Therefore, Al-SiO₂-coated layers produced by magnetron sputtering improve the friction resistance of orthodontic archwires.

The thickness of the coating is an essential factor that is closely related to the expression of torque. The thickness of the coating achieved by the PVD is thinner than that achieved by electroplating and electroless plating [41]. Anuradha et al. [42] reported a uniform, dense titanium coating layer observed by magnetron sputtering, with a thickness ranging from 3–5 µm. Woowa aesthetic archwire has a compound, double-layered coating structure with a silver and platinum coating on the inside and a special polymer coating on the outside with a thickness of 10 µm [42]. Alavi and Hosseini [43] found that the thickness of the epoxy resin coating on G and H1 wire was approximately 0.05 mm. These archwires were used in clinical applications. The thickness of the Al-SiO₂ coating in this experiment is about 1.8 µm, which is obviously less than the thickness of the current clinical aesthetic coatings. Therefore, the Al-SiO₂ coating has little impact on the size of the archwire, and the Al-SiO₂ coating prepared by magnetron sputtering can be used on the surface of orthodontic archwires.

Al-SiO₂-coated archwires have various advantages, including aesthetics, corrosion resistance, bonding strength, and biological safety compared with uncoated archwires. The Al-SiO₂ coating can meet the mechanical properties necessary for orthodontics and match the aesthetics that metal archwires cannot achieve. The newly formed Al-SiO₂-coated layers exhibited a color difference that was nearly identical to that of commercially used coated wires in the clinic. However, the color of the Al-SiO₂-coated layer must be further optimized and validated through fading experiments to better approximate the natural color of the teeth. Because this study was conducted under ideal laboratory conditions, the presence of saliva, plaque, and corrosion in the oral cavity may affect the archwire's performance [44]. Further research is needed to simulate orthodontic tooth movement concerning the clinical scenario for specific evaluation under different situations, focusing on optimizing the Al-SiO₂-coated archwire. Further improvements in the technological parameters and manufacturing technology are needed to increase the bonding force of the coating.

5. Conclusions

This work shows that the stable Al-SiO₂ coatings with strong binding force were successfully fabricated on NiTi and SS archwires by PVDMS. Compared with uncoated

ones, Al–SiO₂ coatings provide better surface smoothness and markedly increase the corrosion resistance of NiTi and SS archwires, which will greatly enhance the efficiency of orthodontic treatment. The Al–SiO₂ coating has no apparent cytotoxicity, indicating the possession of good biocompatibility, while the physicochemical properties of Al–SiO₂ coating markedly improve the aesthetics of the archwires. This Al–SiO₂ coating has excellent potential in orthodontic clinical treatment, which will provide a new idea for the research and development of multifunctional dental biomaterials.

Author Contributions: Conceptualization: H.W.; Data curation: J.Y. and B.Z.; Formal analysis: Y.Y. and H.W.; Investigation: J.Y. and S.M.; Supervision: Y.L.; Writing—original draft: H.W.; Writing—review and editing: S.M., Y.L. and A.L.A. All authors have read and agreed to the published version of the manuscript.

Funding: This work was financially supported by the Shenyang Young and middle-aged Scientific and technological Innovation Talents Support Program (RC210001), the Liaoning Province Key Research and Development Guidance Plan Project (Grant No. 2020JH2/10300038), and the Shenyang Science and Technology Project (20-205-4-099).

Institutional Review Board Statement: Not applicable.

Informed Consent Statement: Not applicable.

Data Availability Statement: Not applicable.

Acknowledgments: The authors would like to express their thanks to teachers and students in the Experimental Centre of School and Hospital of Stomatology, China Medical University, for their continuous help and support.

Conflicts of Interest: The authors declare no conflict of interest.

References

1. Močnik, P.; Kosec, T. A Critical Appraisal of the Use and Properties of Nickel-Titanium Dental Alloys. *Materials* **2021**, *14*, 7859. [[CrossRef](#)] [[PubMed](#)]
2. Dias, V.; Maciel, H.; Fraga, M.; Lobo, A.O.; Pessoa, R.; Marciano, F.R. Atomic Layer Deposited TiO₂ and Al₂O₃ Thin Films as Coatings for Aluminum Food Packaging Application. *Materials* **2019**, *12*, 682. [[CrossRef](#)] [[PubMed](#)]
3. Chen, L.; Yan, X.; Tan, L.; Zheng, B.; Muhammed, F.K.; Yang, K.; Liu, Y. In vitro and in vivo characterization of novel calcium phosphate and magnesium (CaP-Mg) bilayer coated titanium for implantation. *Surf. Coat. Technol.* **2019**, *374*, 784–796. [[CrossRef](#)]
4. Hosseinzadeh Nik, T.; Hooshmand, T.; Farazdaghi, H.; Mehrabi, A.; Razavi, E.S.E. Effect of chlorhexidine-containing prophylactic agent on the surface characterization and frictional resistance between orthodontic brackets and archwires: An in vitro study. *Prog. Orthod.* **2013**, *14*, 48–55. [[CrossRef](#)]
5. Alsanea, J.A.; Al Shehri, H. Evaluation of Nanomechanical Properties, Surface Roughness, and Color Stability of Esthetic Nickel-Titanium Orthodontic Archwires. *J. Int. Soc. Prev. Community Dent.* **2019**, *9*, 33–39. [[CrossRef](#)]
6. Zhao, Y.; Liu, J.; Zhang, M. Use of silver nanoparticle–gelatin/alginate scaffold to repair skull defects. *Coatings* **2020**, *10*, 948. [[CrossRef](#)]
7. Shirakawa, N.; Iwata, T.; Miyake, S.; Otuka, T.; Koizumi, S.; Kawata, T. Mechanical properties of orthodontic wires covered with a polyether ether ketone tube. *Angle Orthod.* **2018**, *88*, 442–449. [[CrossRef](#)]
8. Doshi, U.H.; Bhad-Patil, W.A. Static frictional force and surface roughness of various bracket and wire combinations. *Am. J. Orthod. Dentofac. Orthop.* **2011**, *139*, 74–79. [[CrossRef](#)]
9. Pezzato, L.; Vranescu, D.; Sinico, M.; Gennari, C.; Settini, A.G.; Pranovi, P.; Brunelli, K.; Dabalà, M. Tribocorrosion Properties of PEO Coatings Produced on AZ91 Magnesium Alloy with Silicate- or Phosphate-Based Electrolytes. *Coatings* **2018**, *8*, 202. [[CrossRef](#)]
10. Rachele Bertolini, S.B.; Bordin, A.; Ghiotti, A.; Pezzato, L.; Dabala, M. Fretting Corrosion Behavior of Additive Manufactured and Cryogenic-Machined Ti6Al4V for Biomedical Applications. *Adv. Eng Mater.* **2016**, *19*, 1500629. [[CrossRef](#)]
11. Abdullah, A.O.; Hui, Y.; Pollington, S.; Muhammed, F.K.; Sun, X.; Liu, Y. Comparative Effectiveness of Multiple Laser Scanning and Conventional Techniques on Zirconia Shear Bond Strength. *Coatings* **2019**, *9*, 422. [[CrossRef](#)]
12. Li, C.-J.; Li, J.-L. Evaporated-gas-induced splashing model for splat formation during plasma spraying. *Surf. Coat. Technol.* **2004**, *184*, 13–23. [[CrossRef](#)]
13. Baxamusa, S.H.; Im, S.G.; Gleason, K.K. Initiated and oxidative chemical vapor deposition: A scalable method for conformal and functional polymer films on real substrates. *Phys. Chem. Chem. Phys.* **2009**, *11*, 5227–5240. [[CrossRef](#)] [[PubMed](#)]
14. Sioshansi, P. Tailoring surface properties by ion implantation. *Mater. Eng.* **1987**, *104*, 19–23.

15. Qadir, M.; Li, Y.; Wen, C. Ion-substituted calcium phosphate coatings by physical vapor deposition magnetron sputtering for biomedical applications: A review. *Acta Biomater.* **2019**, *89*, 14–32. [[CrossRef](#)] [[PubMed](#)]
16. Kao, W.-H.; Su, Y.-L.; Horng, J.-H.; Hsieh, Y.-T. Improved tribological properties, electrochemical resistance and biocompatibility of AISI 316L stainless steel through duplex plasma nitriding and TiN coating treatment. *J. Biomater. Appl.* **2017**, *32*, 12–27. [[CrossRef](#)]
17. Arunkumar, P.; Aarthi, U.; Sribalaji, M.; Mukherjee, B.; Keshri, A.K.; Tanveer, W.H.; Cha, S.-W.; Babu, K.S. Deposition rate dependent phase/mechanical property evolution in zirconia and ceria-zirconia thin film by EB-PVD technique. *J. Alloy. Compd.* **2018**, *76*, 418–427. [[CrossRef](#)]
18. Krishnan, V.; Krishnan, A.; Remya, R.; Ravikumar, K.K.; Nair, S.A.; Shibli, S.M.A.; Varma, H.K.; Sukumaran, K.; Kumar, K.J. Development and evaluation of two PVD-coated β -titanium orthodontic archwires for fluoride-induced corrosion protection. *Acta Biomater.* **2011**, *7*, 1913–1927. [[CrossRef](#)]
19. Harlin, P.; Bexell, U.; Olsson, M. Influence of surface topography of arc-deposited TiN and sputter-deposited WC/C coatings on the initial material transfer tendency and friction characteristics under dry sliding contact conditions. *Surf. Coat. Technol.* **2009**, *203*, 1748–1755. [[CrossRef](#)]
20. Goudarzi, M.; Saviz, S.; Ghoranneviss, M.; Salar Elahi, A. Antibacterial characteristics of thermal plasma spray system. *J. X-ray Sci. Technol.* **2018**, *26*, 509–521. [[CrossRef](#)]
21. Monteiro, O.R. Thin film synthesis by energetic condensation. *Annu. Rev. Mater. Res.* **2000**, *31*, 111–137. [[CrossRef](#)]
22. Kula, K.; Phillips, C.; Gibilaro, A.; Proffit, W.R. Effect of ion implantation of TMA archwires on the rate of orthodontic sliding space closure. *Am. J. Orthod. Dentofac. Orthop.* **1998**, *114*, 577–580. [[CrossRef](#)]
23. Heinrichs, J. Laboratory test simulation of aluminium cold forming: Influence from PVD tool coatings on the tendency to galling. *Surf. Coat. Technol.* **2010**, *204*, 3606–3613. [[CrossRef](#)]
24. Schiller, S.; Goedicke, K.; Reschke, J.; Kirchhoff, V.; Schneider, S.; Milde, F. Pulsed magnetron sputter technology. *Surf. Coat. Technol.* **1993**, *61*, 331–337. [[CrossRef](#)]
25. Ozeki, K.; Yuhta, T.; Aoki, H.; Asaoka, T.; Daisaku, T.; Fukui, Y. Deterioration in the superelasticity of Ti sputter coated on NiTi orthodontic wire. *Bio-Med. Mater. Eng.* **2003**, *13*, 355–362.
26. Krishnan, M.; Saraswathy, S.; Sukumaran, K.; Abraham, K.M. Effect of ion-implantation on surface characteristics of nickel titanium and titanium molybdenum alloy arch wires. *Indian J. Dent. Res.* **2013**, *24*, 411–417. [[CrossRef](#)]
27. Palei, B.B.; Dash, T.; Biswal, S.K. Graphene reinforced aluminum nanocomposites: Synthesis, characterization and properties. *J. Mater. Sci.* **2022**, *57*, 8544–8556. [[CrossRef](#)]
28. Yan, Y.; Zheng, B.; Yassir, L.; Liu, X. D-leucine enhances antibiofilm activity of chlorhexidine against caries-causing streptococcus mutans biofilm. *Int. Biodeterior Biodegradation.* **2021**, *157*, 105135. [[CrossRef](#)]
29. Amaya, S.; Pérez, A.; Guzmán, H.; Espinosa, A.; Motta, G.; Mojica, J.; Plaza-Ruiz, S.P. Changes in the mechanical properties of two nickel-titanium archwires after 3 months of clinical usage. *J. World Fed. Orthod.* **2020**, *9*, 175–180. [[CrossRef](#)]
30. Prioteasa, P.; Ibric, N.; Visan, T. The influence of chemical nature on the corrosion behaviour of some dental alloys in Fusayama-Meyer artificial saliva. *J. Optoelectron. Adv. Mater.* **2007**, *9*, 3405–3410.
31. D’Antò, V.; Rongo, R.; Ametrano, G.; Spagnuolo, G.; Manzo, P.; Martina, R.; Paduano, S.; Valletta, R. Evaluation of surface roughness of orthodontic wires by means of atomic force microscopy. *Angle Orthod.* **2012**, *82*, 922–928. [[CrossRef](#)] [[PubMed](#)]
32. Abdullah, A.O.; Yu, H.; Xudong, S.; Muhammed, F.K.; Pollington, S.; Liu, Y. Comparative in Vitro Evaluation between Zirconia and Veneer Ceramic Materials Using Different Techniques. *J. Mater. Eng. Perform.* **2019**, *28*, 6656–6668. [[CrossRef](#)]
33. Zhang, H.; Guo, S.; Wang, D.; Zhou, T.; Wang, L.; Ma, J. Effects of nanostructured, diamondlike, carbon coating and nitrocarburizing on the frictional properties and biocompatibility of orthodontic stainless steel wires. *Angle Orthod.* **2016**, *86*, 782–788. [[CrossRef](#)] [[PubMed](#)]
34. Mystkowska, J.; Niemirowicz-Laskowska, K.; Łysik, D.; Tokajuk, G.; Dąbrowski, J.R.; Bucki, R. The Role of Oral Cavity Biofilm on Metallic Biomaterial Surface Destruction-Corrosion and Friction Aspects. *Int. J. Mol. Sci.* **2018**, *19*, 743. [[CrossRef](#)] [[PubMed](#)]
35. Meyer, R.D.; Meyer, J.; Taloumis, L.J. Intraoral galvanic corrosion: Literature review and case report. *J. Prosthet. Dent.* **1993**, *69*, 141–143. [[CrossRef](#)]
36. Song, F.; Koo, H.; Ren, D. Effects of Material Properties on Bacterial Adhesion and Biofilm Formation. *J. Dent. Res.* **2015**, *94*, 1027–1034. [[CrossRef](#)] [[PubMed](#)]
37. Katić, V.; Curković, H.O.; Semenski, D.; Baršić, G.; Marušić, K.; Spalj, S. Influence of surface layer on mechanical and corrosion properties of nickel-titanium orthodontic wires. *Angle Orthod.* **2014**, *84*, 1041–1048. [[CrossRef](#)]
38. Kim, H.; Johnson, J.W. Corrosion of stainless steel, nickel-titanium, coated nickel-titanium, and titanium orthodontic wires. *Angle Orthod.* **1999**, *69*, 39–44.
39. Kusy, R.P.; Whitley, J.Q. Friction between different wire-bracket configurations and materials. *Semin. Orthod.* **1997**, *3*, 166–177. [[CrossRef](#)]
40. Rincic Mlinaric, M.; Karlovic, S.; Ciganj, Z.; Acev, D.P.; Pavlic, A.; Spalj, S. Oral antiseptics and nickel-titanium alloys: Mechanical and chemical effects of interaction. *Odontology* **2019**, *107*, 150–157. [[CrossRef](#)]
41. De Albuquerque, C.G.; Correr, A.B.; Venezian, G.C.; Santamaria, M.; Tubel, C.A.; Vedovello, S.A.S. Deflection and Flexural Strength Effects on the Roughness of Aesthetic-Coated Orthodontic Wires. *Braz. Dent. J.* **2017**, *28*, 40–45. [[CrossRef](#)] [[PubMed](#)]

42. Anuradha, P.; Varma, N.K.S.; Balakrishnan, A. Reliability performance of titanium sputter coated Ni-Ti arch wires: Mechanical performance and nickel release evaluation. *Bio-Med. Mater. Eng.* **2015**, *26*, 67–77. [[CrossRef](#)] [[PubMed](#)]
43. Alavi, S.; Hosseini, N. Load-deflection and surface properties of coated and conventional superelastic orthodontic archwires in conventional and metal-insert ceramic brackets. *Dent. Res. J.* **2012**, *9*, 133–138.
44. Pan, X.; Li, Y.; Abdullah, A.O.; Wang, W.; Qi, M.; Liu, Y. Micro/nano-hierarchical structured TiO coating on titanium by micro-arc oxidation enhances osteoblast adhesion and differentiation. *R. Soc. Open Sci.* **2019**, *6*, 182031. [[CrossRef](#)] [[PubMed](#)]